

Organotransition-Metal Metallocarboranes. 46. Multidecker Sandwiches of the Cobalt Group Metals^{†,1}

David A. Franz,[‡] Eric J. Houser, Michal Sabat, and Russell N. Grimes*

Department of Chemistry, University of Virginia, Charlottesville, Virginia 22901

Received May 31, 1996[⊗]

The double-decker sandwich complex Cp*Ir(2,3-Et₂C₂B₄H₄) (**1a**) was prepared via deprotonation of *nido*-2,3-Et₂C₂B₄H₆ to its mono- or dianion and reaction with (Cp*IrCl₂)₂ in THF and isolated as a colorless air-stable solid; the *B*(4)-chloro derivative **1b** was also obtained. Decapitation of **1a** and **1b** with TMEDA afforded colorless *nido*-Cp*Ir(2,3-Et₂C₂B₃H₅) (**2a**) and its 4-chloro derivative **2b**. Chlorination of **1a** by Cl₂ or *N*-chlorosuccinimide gave the symmetrical species Cp*Ir(2,3-Et₂C₂B₄H₃-5-Cl) (**1c**), which was decapped to yield *nido*-Cp*Ir(2,3-Et₂C₂B₃H₄-5-Cl) (**2c**). The triple-decker complexes Cp*Ir(2,3-Et₂C₂B₃H₂-4[6]-Cl)IrCp* (**3**), an orange solid, and dark green Cp*Ir(2,3-Et₂C₂B₃H₂-4[6]-Cl)CoCp* (**5**) were prepared from **2a** and *nido*-Cp*Co(2,3-Et₂C₂B₃H₅) (**4a**), respectively, by deprotonation and reaction with (Cp*IrCl₂)₂ in THF. Reaction of the **2c**⁻ anion with Rh(MeCN)₃-Cl₃ gave the dark green tetradecker complex [Cp*Ir(Et₂C₂B₃H₂-5-Cl)]₂RhH (**6**). In an attempt to prepare a heterotrimetallic Co–Rh–Ir tetradecker sandwich, a three-way reaction involving the deprotonated anions derived from Cp*Co(2,3-Et₂C₂B₃H₄-5-Cl) (**4b**) and **2c** with Rh(MeCN)₃Cl₃ was conducted. The desired species Cp*Co(Et₂C₂B₃H₂Cl)RhH(Et₂C₂B₃H₂Cl)IrCp* (**7**) and the tetradeckers [Cp*Co(Et₂C₂B₃H₂Cl)]₂RhH (**8**) and **6** were isolated in small quantities from the product mixture; many other apparent triple-decker and tetradecker products were detected via mass spectroscopy but were not characterized. All new compounds were isolated via column or plate chromatography and characterized via NMR, UV–visible, and mass spectroscopy and by X-ray crystal structure determinations of **1a** and **3**. Crystal data for **1a**: space group *C2/c*; *a* = 28.890(5) Å, *b* = 8.511(2) Å, *c* = 15.698(4) Å, β = 107.61(2)°; *Z* = 8; *R* = 0.049 for 1404 independent reflections having *I* > 3σ(*I*). Crystal data for **3**: space group *P2₁/c*; *a* = 11.775(4) Å, *b* = 15.546(5) Å, *c* = 15.500(5) Å, β = 103.16(3)°; *Z* = 4; *R* = 0.066 for 2635 independent reflections having *I* > 3σ(*I*).

Introduction

Studies of cobaltacarborane sandwich complexes composed of CoC₂B₃ and/or CoC₂B₄ cluster units have led to a multiplicity of structurally varied compound types, including triple-decker and tetra-, penta-, and hexadecker sandwiches, linked-sandwich oligomers, B–B- and C–C-connected dimers, metallocene–metallocarborane salts, hydridocobaltacarboranes, Fischer carbenes, and other classes.^{1b,2} Other transition metals, e.g., Fe, Ni, Ru, Rh, Os, Ir, and Pt, have been incorporated into some of these cobaltacarborane systems. However, the synthetic rock on which most of this chemistry has been built is the extremely robust and versatile double-decker complex Cp*Co(2,3-Et₂C₂B₄H₄) (Cp* = η⁵-C₅Me₅), an orange air-stable solid, and its “decapitated” derivative, yellow, air-stable *nido*-Cp*Co(2,3-Et₂C₂B₃H₅).³ The ease of preparation of these building-block compounds, allowing their synthesis in 10–20 g lots, has made it possible to develop this chemistry in some depth over the last 7 years.

Isoelectronic complexes of iron and ruthenium, e.g. (arene)M-(Et₂C₂B₄H₄) (M = Fe, Ru), and their decapped counterparts, *nido*-(arene)M(Et₂C₂B₃H₅), have also been investigated to a lesser degree⁴ and have led, for example, to the synthesis and characterization of several Ru–M–Ru tetradecker systems in which M is Co or Ni.⁵ We were, however, intrigued by the possibilities that might be afforded by the heavier group 9 congeners of cobalt, both in a fundamental sense (How would formal replacement of Co by Rh or Ir affect the electronic and other properties of these systems?) and also from the more practical viewpoint that irida- and rhodacarborane sandwich complexes might offer advantages in the development of new electroactive materials and catalysts. Rhodium double-decker, triple-decker, and tetradecker sandwiches containing pyramidal Et₂C₂B₄H₄²⁻ or planar Et₂C₂B₃H_nⁿ⁻⁷ (*n* = 3, 5) ligands have been characterized,⁶ but no iridium complexes of these (or other) small-carborane ligands have been reported. However, iridacarboranes incorporating 9-vertex IrCB₇⁷ and 10-vertex IrC₂B₈⁸ clusters are known, as are larger species having up to 13 vertices^{2a}). Here we report some exploratory studies in small iridacarborane chemistry involving all three group 9 metals.

[†] Dedicated to Professor Walter Siebert on the occasion of his 60th birthday.

[‡] Visiting Professor, 1994–5, on leave from the Department of Chemistry, Lycoming College, Williamsport, PA.

[⊗] Abstract published in *Advance ACS Abstracts*, November 1, 1996.

(1) (a) Part 45: Houser, E. J.; Curtis, M. A.; Sabat, M.; Grimes, R. N. *J. Organomet. Chem.*, in press. (b) Part 44: Wang, X.; Sabat, M.; Grimes, R. N. *J. Am. Chem. Soc.* **1995**, *117*, 12227.

(2) For recent reviews see: (a) Grimes, R. N. In *Comprehensive Organometallic Chemistry II*; Abel, E., Stone, F. G. A., Wilkinson, G., Eds.; Pergamon Press: Oxford, England, 1995; Vol. 1, Chapter 9, pp 373–430. (b) Hosmane, N. S.; Maguire, J. A. *J. Cluster Sci.* **1993**, *4*, 297. (c) Grimes, R. N. *Chem. Rev.* **1992**, *92*, 251. (d) Grimes, R. N. In *Current Topics in the Chemistry of Boron*; Kabalka, G. W., Ed.; Royal Society of Chemistry: London, 1994; p 269.

(3) Davis, J. H., Jr.; Sinn, E.; Grimes, R. N. *J. Am. Chem. Soc.* **1989**, *111*, 4776.

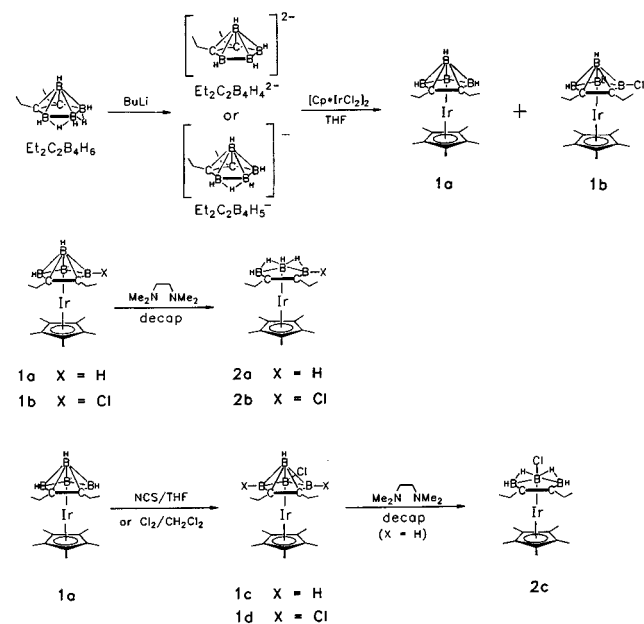
(4) (a) Davis, J. H., Jr.; Attwood, M. D.; Grimes, R. N. *Organometallics* **1990**, *9*, 1171. (b) Attwood, M. D.; Davis, J. H., Jr.; Grimes, R. N. *Organometallics* **1990**, *9*, 1177.

(5) Greiwe, P.; Sabat, M.; Grimes, R. N. *Organometallics* **1995**, *14*, 3683.

(6) (a) Fessenbecker, A.; Attwood, M. D.; Bryan, R. F.; Grimes, R. N.; Woode, M. K.; Stephan, M.; Zenneck, U.; Siebert, W. *Inorg. Chem.* **1990**, *29*, 5157. (b) Fessenbecker, A.; Attwood, M. D.; Grimes, R. N.; Stephan, M.; Pritzkow, H.; Zenneck, U.; Siebert, W. *Inorg. Chem.* **1990**, *29*, 5164. (c) Müller, P. Ph.D. Thesis, University of Heidelberg, 1994. Müller, P.; Pritzkow, H.; Grimes, R. N.; Siebert, W. To be published.

(7) Stibr, B.; Kennedy, J. D.; Drdakova, E.; Thornton-Pett, M. *J. Chem. Soc., Dalton Trans.* **1994**, 229.

Scheme 1



Results and Discussion

Synthesis and Reactions of Small Iridacarboranes. As an entry to this area, the double-decker complex Cp*Ir(2,3-Et₂C₂B₄H₄) (**1a**) was prepared from the carborane monoanion or dianion (both generated by deprotonation of *nido*-2,3-Et₂C₂B₄H₆ via reaction with the dimer (Cp*IrCl₂)₂ in THF (Scheme 1). Compound **1a** was isolated as air-stable colorless crystals and characterized from ¹H, ¹¹B, and ¹³C NMR, UV-visible, and mass spectra and X-ray crystallography. The yields were variable but were generally higher in syntheses involving the monoanion (30–50%) than in those where the dianion was employed (17–20%). In the monoanion experiments, chlorination at boron occurred to give the 4-chloro derivative (**1b**) as a side product; with the dianion, **1b** was observed in some but not all runs (the formation of **1b** was observed even when no chlorinated solvents were employed during workup). When recrystallized (Cp*IrCl₂)₂ was used in an attempt to eliminate traces of IrCl₃ in the system, essentially no **1b** was formed from the dianion, although this product was still obtained in small amounts in monoanion reactions. When present, **1b** (also colorless and air-stable) was easily separated from **1a** by preparative chromatography on silica.

The NMR spectra of both compounds, the data for which are listed in Table 1 and the Experimental Section, are consistent with the structures shown. Thus, the parent species **1a** shows mirror symmetry, and the absence of symmetry in **1b**, with four inequivalent boron atoms, establishes the location of chlorine on B(4)/B(6). The formation of **1b** contrasts sharply with the radical halogenation of **1a** and other *closo*-MC₂B₄ clusters, which generates exclusively *B*(5)-halo derivatives (see below). The chlorination of **1a** in the presence of the dichloroiridium reagent obviously involves a different mechanism, but this question was not further investigated.

The X-ray structure determination of **1a**, which is the first small iridacarborane to be crystallographically characterized, is of interest mainly in its relation to related Co and Rh

Table 1. FT NMR Data

compd	300-MHz ¹ H NMR Data		
	δ ^{a,b}		
1a (CDCl ₃)	2.29 m (CH ₂), 1.97 s (Cp*), 1.20 t (CH ₃)		
1a (C ₆ D ₆)	2.14 m (CH ₂), 1.65 s (Cp*), 1.23 t (CH ₃)		
1b (CDCl ₃)	2.59 m (CH ₂), 2.29 m (CH ₂), 2.18 m (CH ₂), 1.94 s (Cp*), 1.21 t (CH ₃), 1.05 t (CH ₃)		
1c (CDCl ₃)	2.3 m (CH ₂), 2.1 m (CH ₂), 1.97 s (Cp*), 1.17 t (CH ₃)		
1d (CDCl ₃)	2.5 m (CH ₂), 2.2 m (CH ₂), 1.91 s (Cp*), 1.13 t (CH ₃)		
2a (CDCl ₃)	2.01 m (CH ₂), 1.96 s (Cp*), 1.78 m (CH ₂), 1.13 t (CH ₃), -6.3 br (BHB)		
2a (C ₆ D ₆)	2.1 m (CH ₂), 1.9 (CH ₂), 1.73 s (Cp*), 1.32 t (CH ₃), -5.8 br (BHB)		
2b (CDCl ₃)	2.1 m (CH ₂), 1.91 s (Cp*), 1.8 m (CH ₂), 1.14 t (CH ₃), -4.2 br (BHB), -6.0 br (BHB)		
2b (C ₆ D ₆)	2.2 m (CH ₂), 2.0 m (CH ₂), 1.8 m (CH ₂), 1.7 m (CH ₂), 1.65 s (Cp*), 1.33 t (CH ₃), 1.27 (CH ₃), -3.8 br (BHB), -5.7 br (BHB)		
2c (CDCl ₃)	2.3 m (CH ₂), 2.0 m (CH ₂), 1.93 s (Cp*), 1.76 m (CH ₂), 1.71 m (CH ₂), 1.11 t (CH ₃), -4.1 br (BHB)		
3 (CDCl ₃)	2.43 m (CH ₂), 1.75 s (Cp*), 1.162/1.154 ^c t (CH ₃)		
3 (C ₆ D ₆)	2.5 m (CH ₂), 1.65 s (Cp*), 1.334/1.307 ^c t (CH ₃)		
5 (CDCl ₃)	2.74 m (CH ₂), 2.40 m (CH ₂), 1.74 s (Cp*Ir), 1.63 s (Cp*Co), 1.256/1.251 ^c t (CH ₃)		
5 (C ₆ D ₆)	2.9 m (CH ₂), 2.7 m (CH ₂), 2.5 m (CH ₂), 2.4 m (CH ₂), 1.63 s (Cp*), 1.60 s (Cp*), 1.403/1.392 ^c t (CH ₃)		
6 (CDCl ₃)	2.4 m (CH ₂), 2.1 m (CH ₂), 1.74 s (Cp*), 1.27 t (CH ₃), -4.4 br (RhH)		
6 (C ₆ D ₆)	2.7 m (CH ₂), 2.1 m (CH ₂), 1.54 t (CH ₃), 1.47 s (Cp*), -4.0 br (RhH)		
7 (CDCl ₃)	1.9 m (CH ₂), 1.73 s (Cp*Ir), 1.60 (Cp*Co), 1.43 t (CH ₃), 1.21 (CH ₃) - 2.8 br (RhH)		
8 (CDCl ₃)	1.57 s (Cp*), 1.37 t (CH ₃), -1.6 br (RhH)		

115.8-MHz ¹¹B NMR Data

compd	δ ^{d,e}	rel areas
1a	19.9 (153) [B(7)], 10.7 (138) [B(5)], 7.2 (145) [B(4,6)]	1:1:2
1b	8.6 (169) [B(7)], 6.6 [B(4)], -3.2 (177) [B(5 or 6)], -5.1 (173) [B(6 or 5)]	1:1:1:1
2a^f	0.52 ^g (153, J _{BH(term)}); 41, J _{BH(bridge)} [B(5)], -3.40 ^h (147, J _{BH(term)}); 33, J _{BH(bridge)} [B(4,6)]	1:2
2b	5.3 (34, J _{BH(bridge)}) [B(4)], -2.4 (160) [B(5 or 6)], -6.3 (159) [B(6 or 5)]	1:1:1
3	14.6 (112) [B(5 or 6)], 0.7 [B(4)], -9.1 (103) [B(6 or 5)]	1:1:1
5	31.4 (90) [B(5 or 6)], 8.5 [B(4)], 1.2 (105) [B(6 or 5)]	1:1:1

^a Shifts relative to (CH₃)₄Si. Integrated peak areas in all cases are consistent with the assignments given. Key: br = broad, m = multiplet, s = singlet, d = doublet, t = triplet, q = quartet. ^b B-H_{terminal} resonances are broad quartets and mostly obscured by other signals. ^c Overlapped triplets. ^d Shifts relative to BF₃·OEt₂; positive values downfield. H-B coupling constants (Hz) are given in parentheses when resolved. ^e CH₂Cl₂ solution. ^f Hexane solution. ^g Doublet of triplets. ^h Doublet of doublets.

carborane complexes. Although some apparent disorder was encountered in the Cp* ligand, the essential features of the structure were established. The molecular geometry is depicted in Figure 1, with data collection parameters listed in Table 2 and bond distances and angles in Table 3. The Ir-C, Ir-B, and B-C bond lengths in the IrC₂B₄ cluster are all within normal ranges and compare closely with those in CoC₂B₄ and RhC₂B₄ clusters, taking into account the larger covalent radii of Rh and Ir compared to Co. Thus, the Ir atom in **1a** is located 1.724 and 1.826 Å, respectively, from the C₂B₃ and Cp* ring planes; the corresponding distances in 5,5'-[Cp*Co(2,3-Et₂C₂B₄H₃)₂] are 1.574 and 1.651 Å.⁹ In the nearest structurally characterized rhodacarborane analogue, (Et₂C₂B₄H₄)Rh(Et₂-MeC₃B₂Et₂)CoCp, the rhodium atom is 1.76 and 1.80 Å, respectively, from the carborane and C₃B₂ ring planes.^{6a} The two ring planes in **1a** are virtually parallel, with a dihedral angle of 1.95°; this is closely comparable to the 5,5'-[Cp*Co-(Et₂C₂B₄H₃)₂] dimer⁹ in which the angle is 0.2°.

(8) (a) Crook, J. E.; Greenwood, N. N.; Kennedy, J. D.; McDonald, W. S. *J. Chem. Soc., Chem. Commun.* **1981**, 933. (b) Crook, J. E.; Greenwood, N. N.; Kennedy, J. D.; McDonald, W. S. *J. Chem. Soc., Chem. Commun.* **1983**, 83. (c) Alcock, N. W.; Taylor, J. G.; Wallbridge, M. G. H. *Acta Crystallogr.* **1988**, C4, 2079.

(9) Wang, X.; Sabat, M.; Grimes, R. N. *Organometallics* **1995**, 14, 4668.

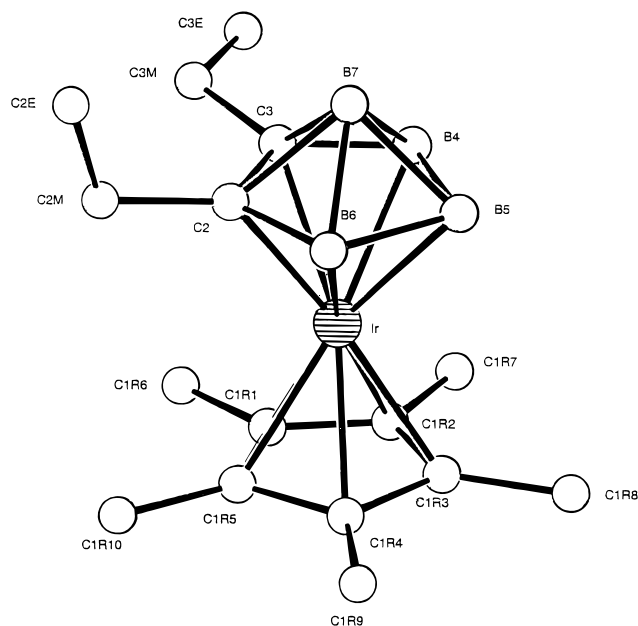


Figure 1. Molecular structure of $\text{Cp}^*\text{Ir}(2,3\text{-Et}_2\text{C}_2\text{B}_4\text{H}_4)$ (**1a**) showing non-hydrogen atoms.

Table 2. Experimental X-ray Diffraction Parameters and Crystal Data

	1a	3
empirical formula	$\text{IrC}_{16}\text{B}_4\text{H}_{29}$	$\text{Ir}_2\text{ClC}_{26}\text{B}_3\text{H}_{42}$
fw	456.9	806.9
crystal color, habit	colorless needle	colorless block
crystal dimens, mm	$0.24 \times 0.22 \times 0.41$	$0.32 \times 0.20 \times 0.46$
space group	$C2/c$	$P2_1/c$
a , Å	28.890(5)	11.775(4)
b , Å	8.511(2)	15.546(5)
c , Å	15.698(4)	15.500(5)
β , deg	107.61(2)	103.16(3)
V , Å ³	3679(3)	2758(3)
Z	8	4
μ , cm^{-1} (Mo $K\alpha$)	72.22	97.18
transm factors	0.13–1.00	0.23–1.00
D (calcd), g cm^{-3}	1.65	1.94
$2\theta_{\text{max}}$, deg	46.0	46.0
no. of reflns measd	2770	4006
no. of reflns obsd ($I > 3\sigma(I)$)	1404	2635
R	0.049	0.066
R_w	0.061	0.091
largest peak in final diff map, $\text{e}/\text{Å}^3$	3.8 (close to Ir)	2.1 (close to Ir(2))

Decapitation and Chlorination of 1a and 1b. Treatment of **1a** with wet TMEDA in the usual manner^{1b,2c,d} afforded *nido*- $\text{Cp}^*\text{Ir}(2,3\text{-Et}_2\text{C}_2\text{B}_3\text{H}_5)$ (**2a**), which was obtained, following workup, as a colorless crystalline solid and characterized spectroscopically (Table 1 and Scheme 1). The proton-coupled ¹¹B NMR spectrum is unusually well resolved, with the usual $\text{B-H}_{\text{terminal}}$ doublets exhibiting further splitting arising from coupling to adjacent bridging hydrogens: thus, the signal of B(5), which is coupled to both BHB protons, appears as a doublet of triplets, while the B(4,6) resonance (coupled to only one BHB) is seen as a doublet of doublets. The 4-chloro derivative **1b** was similarly decapped (in mixtures of **1a** and **1b**) to yield **2b**, as shown. The asymmetric B(4/6)–Cl structure of **2b** is indicated by the ¹¹B NMR data, which show three inequivalent resonances, as well as the ¹H spectrum, which shows two well-separated B–H–B high-field signals. The B(4)–Cl singlet resonance in the ¹¹B spectrum shows B–H_{bridge} coupling, but no such feature is seen in the B(5)–H and B(6)–H doublets.

Table 3. Bond Distances and Selected Bond Angles for $\text{Cp}^*\text{Ir}(2,3\text{-Et}_2\text{C}_2\text{B}_4\text{H}_4)$ (**1a**)

Bond Distances, Å			
Ir–C(2)	2.16(2)	C(3)–B(4)	1.54(3)
Ir–C(3)	2.16(2)	C(3)–B(7)	1.79(3)
Ir–C(1R1)	2.22(2)	C(1R1)–C(1R2)	1.41(3)
Ir–C(1R2)	2.21(2)	C(1R1)–C(1R5)	1.45(3)
Ir–C(1R3)	2.17(2)	C(1R1)–C(1R6)	1.50(3)
Ir–C(1R4)	2.20(2)	C(1R2)–C(1R3)	1.44(3)
Ir–C(1R5)	2.20(2)	C(1R2)–C(1R7)	1.48(2)
Ir–B(4)	2.20(2)	C(1R3)–C(1R4)	1.45(3)
Ir–B(5)	2.26(2)	C(1R3)–C(1R8)	1.50(3)
Ir–B(6)	2.22(2)	C(1R4)–C(1R5)	1.43(3)
C(2)–C(2M)	1.53(3)	C(1R4)–C(1R9)	1.50(3)
C(2)–C(3)	1.51(3)	C(1R5)–C(1R10)	1.50(3)
C(2)–B(6)	1.55(3)	B(4)–B(5)	1.72(3)
C(2)–B(7)	1.77(3)	B(4)–B(7)	1.80(3)
C(2M)–C(2E)	1.48(3)	B(5)–B(6)	1.74(3)
C(3M)–C(3)	1.51(3)	B(5)–B(7)	1.76(3)
C(3M)–C(3E)	1.50(3)	B(6)–B(7)	1.80(3)

Selected Bond Angles, deg			
Ir–C(2)–C(2M)	133(2)	C(2)–B(6)–B(5)	105(2)
C(2M)–C(2)–C(3)	122(2)	C(2)–C(3)–C(3M)	119(2)
C(2M)–C(2)–B(6)	124(2)	C(2)–C(3)–B(4)	112(3)
C(3)–C(2)–B(6)	113(2)	C(3M)–C(3)–B(4)	128(2)
C(2M)–C(2)–B(7)	134(2)	C(3M)–C(3)–B(7)	135(2)
Ir–C(3)–C(3M)	132(2)	C(2)–C(2M)–C(2E)	112(2)
C(3)–B(4)–B(5)	107(2)	C(3)–C(3M)–C(3E)	117(2)
B(4)–B(5)–B(6)	103(2)		

Since the formation of tetradecker sandwiches via stacking of MC_2B_3 cluster units with metal ions is facilitated by electron-withdrawing substituents at B(5) on the open face,¹⁰ we converted **1a** in two stages to an open-faced B(5)-chloro derivative that was employed for tetradecker synthesis as described below. Chlorination of **1a** was achieved via reaction with Cl_2 or *N*-chlorosuccinimide (NCS), both procedures generating the symmetrical monochloro isomer $\text{Cp}^*\text{Ir}(2,3\text{-Et}_2\text{C}_2\text{B}_4\text{H}_3\text{-5-Cl})$ (**1c**) as the major product; in the Cl_2 reaction, a small quantity of a dichlorinated product was also obtained. When a higher concentration of Cl_2 was employed, the trichlorinated species **1d** was isolated and characterized (Scheme 1). The more convenient synthesis of **1c** was that employing NCS, which gave the desired product in nearly pure form. The proposed structures of **1c** and **1d** (both colorless solids) are supported by their ¹H NMR and mass spectra and also, in the case of **1c**, by the geometry of its decapped derivative *nido*- $\text{Cp}^*\text{Ir}(\text{Et}_2\text{C}_2\text{B}_3\text{H}_4\text{-5-Cl})$ (**2c**). The latter compound was generated from **1c** by treatment with TMEDA, which gave **2c** as a white solid in an isolated yield of 74–76% for the overall **1a**–**2c** conversion. That **2c** and **1c** are substituted at the middle boron [B(5)] is clear from their NMR spectra, which show unique ethyl and B–H–B resonances and are distinct from those of their respective B(4/6)–Cl isomers **1b** and **2b**.

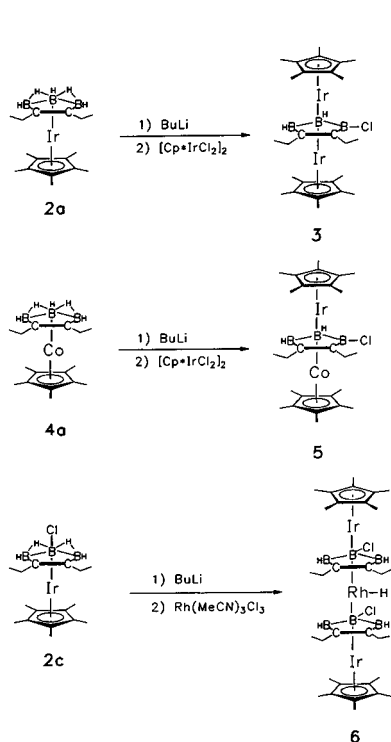
The formation of **1c** parallels the previously studied halogenation of the analogous cobalt complex $\text{Cp}^*\text{Co}(\text{Et}_2\text{C}_2\text{B}_4\text{H}_4)$ by *N*-halosuccinimides,¹¹ which similarly effected regiospecific Cl-, Br-, or I-monosubstitution at B(5).

Synthesis of Iridacarborane Triple-Decker Complexes. The double-decker complex **2a** was bridge-deprotonated with *n*-butyllithium, and the resulting monoanion was treated with $(\text{Cp}^*\text{IrCl}_2)_2$ in THF solution to give, following chromatographic separation on silica, orange $\text{Cp}^*\text{Ir}(2,3\text{-Et}_2\text{C}_2\text{B}_3\text{H}_2\text{-4[6-Cl]})\text{IrCp}^*$ (**3**) in 41% isolated yield (Scheme 2).

(10) Piegras, K. W.; Meng, X.; Hölscher, M.; Sabat, M.; Grimes, R. N. *Inorg. Chem.* **1992**, *31*, 5202.

(11) Stockman, K. E.; Garrett, D. L.; Grimes, R. N. *Organometallics* **1995**, *14*, 4661.

Scheme 2



The characterization of **3** was straightforward, on the basis of its ^1H and ^{11}B NMR, UV–visible, and mass spectra. The asymmetry of **3**, clearly evident in the NMR data, reveals that the Cl substituent is on B(4/6) rather than the central boron [B(5)], an assignment that was subsequently confirmed crystallographically as discussed below. Although about 50% of the neutral starting complex **2a** was recovered, **3** was the only product isolated from this reaction, even when a variety of solvent mixtures were employed as eluents in chromatography. Except for minor peaks in the mass spectrum of **3**, which could well arise from fragmentation of the parent species, no evidence was seen for the parent (unchlorinated) triple-decker or for any chloro derivatives. The source of the chlorine in **3** is clearly the iridium reagent, since TLC analysis of the reaction mixture prior to workup in CH_2Cl_2 confirmed the presence of **3** at that stage. Hence it appears that any parent triple-decker that forms in the reaction is rapidly and regioselectively chlorinated at the B(4/6) position.

The UV–visible spectrum of **3** exhibits two very intense absorptions at λ 234 nm (ϵ 26 000 $\text{cm}^{-1} \text{M}^{-1}$) and 272 nm (ϵ 41 000 $\text{cm}^{-1} \text{M}^{-1}$), assigned to d–d charge-transfer excitations involving the iridium atoms. This strong metal–metal interaction is underlined by the contrast between this deeply colored species and its colorless monometallic precursor **2a** and in this respect is similar to previously studied C_2B_3 -bridged Co–M–Co tetradecarboranes¹⁰ where M is Co, Ni, or Ru, as well as penta- and hexadecarborane sandwiches involving Co and Ni.^{1b} The fact that **3**, a bimetallic complex, exhibits absorption intensities comparable to those of the larger multimetal sandwiches is remarkable and merits further study.

The major absorption maxima in **3** are somewhat blue-shifted relative to those of carborane-bridged multideckers of first-row transition metals, which appear at λ 330–380 nm (in CH_2Cl_2 or CHCl_3) for triple-deckers,¹² 350–440 nm for tetradecarboranes,¹⁰ and 390–410 nm for penta- and hexadecarboranes.^{1b} This is not unexpected, since Co–Ru triple-deckers show their strongest

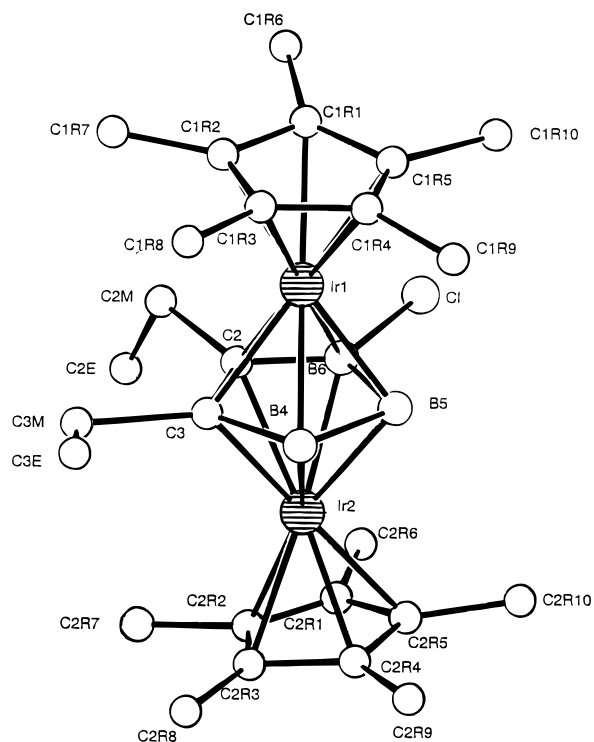


Figure 2. Molecular structure of $\text{Cp}^*\text{Ir}(2,3\text{-Et}_2\text{C}_2\text{B}_3\text{H}_2\text{-6-Cl})\text{IrCp}^*$ (**3**) showing non-hydrogen atoms.

absorptions at lower wavelengths (ca. 280–294 nm),^{3,12,13} owing to the larger d–d separations arising from higher-energy d levels present in the second-row transition metal Ru. In the Ru–Ru triple-decker $(\text{Me}_2\text{CHC}_6\text{H}_4\text{Me})_2\text{Ru}_2(\text{Et}_2\text{C}_2\text{B}_3\text{H}_3)$, the maximum absorption is lower still, at 260 nm;³ thus, the even lower-wavelength bands observed for **3** represent an extension of this trend to a third-row metal sandwich system.

A heterodimetallic Co–Ir counterpart of **3** was prepared via reaction of the *nido*- $\text{Cp}^*\text{Co}(\text{Et}_2\text{C}_2\text{B}_3\text{H}_4)^-$ anion (**4a**[−]) with $(\text{Cp}^*\text{IrCl}_2)_2$, affording green crystalline $\text{Cp}^*\text{Ir}(\text{Et}_2\text{C}_2\text{B}_3\text{H}_2\text{-4(6-Cl)})\text{CoCp}^*$ (**5**) in 50% isolated yield (Scheme 2). The geometry shown is consistent with NMR and mass spectra, and it is apparent that the structure is analogous to that of **3**; thus, the ^1H and ^{11}B NMR patterns point to chlorine substitution at B(4/6) rather than B(5). The UV–visible spectrum is also similar to that of **3**, but significantly the most intense peak occurs at λ 326 nm (ϵ 38 000 $\text{cm}^{-1} \text{M}^{-1}$), representing a lower-energy d–d transition compared to that for **3**. This is as expected for a Co–Ir compared to an Ir–Ir system, but it is also substantially red-shifted compared to those for the Co–Ru triple-deckers mentioned earlier.

X-ray Diffraction Study of 3. A crystallographic structure determination established the triple-decker geometry pictured in Figure 2, with relevant data collected in Tables 2 and 4.

The observed bond lengths and angles are typical for multidecker metallacarborane sandwiches containing C_2B_3 carborane bridging rings. However, **3** is the first such complex containing exclusively third-row transition metals, and the large Ir–Ir separation of 3.46 Å may be compared to the M–M' distances (ca. 3.15–3.30 Å) in multideckers where M and M' are first-row metals.^{1b,3,5,10,12} In the one prior structurally characterized example having two non-first-row transition metals bridged by a C_2B_3 ring,³ $(\text{Me}_2\text{CHC}_6\text{H}_4\text{Me})_2\text{Ru}_2(\text{Et}_2\text{C}_2\text{B}_3\text{H}_3)$, the Ru–Ru distance is 3.48 Å, nearly identical to that in **3**.

(12) Wang, X.; Sabat, M.; Grimes, R. N. *J. Am. Chem. Soc.* **1995**, *117*, 12218.

(13) Merkert, J.; Davis, J. H., Jr.; Geiger, W.; Grimes, R. N. *J. Am. Chem. Soc.* **1992**, *114*, 9846.

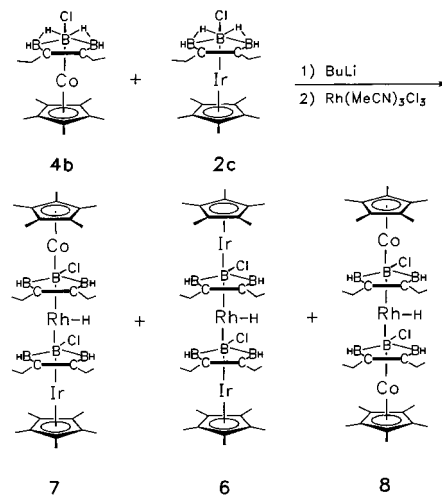
Table 4. Bond Distances and Selected Bond Angles for Cp*Ir(Et₂C₂B₃H₂-4[6]-Cl)IrCp*³ (3)

Bond Distances, Å			
Ir(1)–C(2)	2.20(2)	C(3M)–C(3)	1.82(4)
Ir(1)–C(3)	2.21(3)	C(3M)–C(3E)	0.81(4)
Ir(1)–C(1R1)	2.16(3)	C(3)–B(4)	1.61(4)
Ir(1)–C(1R2)	2.18(3)	C(1R1)–C(1R2)	1.46(4)
Ir(1)–C(1R3)	2.10(3)	C(1R1)–C(1R5)	1.48(4)
Ir(1)–C(1R4)	2.13(3)	C(1R1)–C(1R6)	1.61(6)
Ir(1)–C(1R5)	2.15(3)	C(1R2)–C(1R3)	1.26(4)
Ir(1)–B(4)	2.18(3)	C(1R2)–C(1R7)	1.52(5)
Ir(1)–B(5)	2.15(3)	C(1R3)–C(1R4)	1.42(4)
Ir(1)–B(6)	2.19(3)	C(1R3)–C(1R8)	1.61(6)
Ir(2)–C(2)	2.19(2)	C(1R4)–C(1R5)	1.18(4)
Ir(2)–C(3)	2.14(3)	C(1R4)–C(1R9)	1.62(5)
Ir(2)–C(2R1)	2.23(3)	C(1R5)–C(1R10)	1.72(6)
Ir(2)–C(2R2)	2.24(3)	C(2R1)–C(2R2)	1.30(4)
Ir(2)–C(2R3)	2.15(3)	C(2R1)–C(2R5)	1.36(4)
Ir(2)–C(2R4)	2.10(2)	C(2R1)–C(2R6)	1.60(5)
Ir(2)–C(2R5)	2.15(3)	C(2R2)–C(2R3)	1.30(4)
Ir(2)–B(4)	2.21(3)	C(2R2)–C(2R7)	1.65(5)
Ir(2)–B(5)	2.14(2)	C(2R3)–C(2R4)	1.51(3)
Ir(2)–B(6)	2.13(3)	C(2R3)–C(2R8)	1.72(6)
Cl–B(6)	1.95(3)	C(2R4)–C(2R5)	1.47(4)
C(2)–C(2M)	1.70(4)	C(2R4)–C(2R9)	1.54(4)
C(2)–C(3)	1.42(4)	C(2R5)–C(2R10)	1.54(4)
C(2)–B(6)	1.41(3)	B(4)–B(5)	1.68(4)
C(2M)–C(2E)	1.42(4)	B(5)–B(6)	1.61(4)

Selected Bond Angles, deg			
Ir(1)–C(2)–C(2M)	122(2)	C(2)–C(3)–B(4)	113(2)
Ir(2)–C(2)–C(2M)	134(2)	C(3M)–C(3)–B(4)	124(2)
C(2M)–C(2)–C(3)	126(2)	C(3)–B(4)–B(5)	100(2)
C(2M)–C(2)–B(6)	121(2)	B(4)–B(5)–B(6)	104(2)
C(3)–C(2)–B(6)	113(2)	Cl–B(6)–C(2)	129(2)
C(2)–C(2M)–C(2E)	110(3)	Cl–B(6)–B(5)	121(2)
C(3)–C(3M)–C(3E)	108(4)	C(2)–B(6)–B(5)	110(2)
Ir(1)–C(3)–C(3M)	123(2)	Ir(1)–B(6)–Cl	124(1)
Ir(2)–C(3)–C(3M)	132(2)	Ir(2)–B(6)–Cl	129(1)
C(2)–C(3)–C(3M)	122(2)		

The other noteworthy feature in **3** is the degree of bending, marked by a dihedral angle of 17° between the end Cp* ring planes, which is atypically large for triple-decker sandwiches having no metal-bound substituents between the rings (angles of ca. 12° are commonly observed in carborane-bridged triple-deckers³). As earlier papers from this laboratory have noted,^{1b,10} the bending of C₂B₃-bridged multiple-decker stacks is primarily of electronic rather than steric origin and is attributed to inequivalence in the binding of metal atoms to carbon vs boron atoms in the rings. In the case of **3**, it is likely that a strong Ir–Ir interaction (vide supra) is involved, since maximum overlap of the metal hybrid orbitals (e.g., d_{z²}p_z) may favor a tilted orientation.

Synthesis of Rhodium-Centered Tetradecker Complexes. The B(5)-chlorinated iridacarborane double-decker complex **2c** was employed as a synthon to construct tetradeckers via deprotonation to generate the anion, followed by reaction with tris(acetonitrile)rhodium(III) chloride (Scheme 2, bottom). This approach gave a mixture of tetradecker products in low individual yields, the total yield corresponding to 24% based on starting complex consumed. Chromatography on silica using a series of solvent mixtures (see Experimental Section) afforded several products that were identified from their mass spectra as chlorinated tetradeckers, including the desired B(5),B(5')-dichloro complex **6** as well as a monochloro and a trichloro derivative of this same tetradecker sandwich system. The main product, [Cp*Ir(Et₂C₂B₃H₂-5-Cl)]₂RhH (**6**) was obtained as a diamagnetic dark green solid and characterized via NMR, UV–visible, and mass spectra. The proposed geometry is supported by the simple proton NMR spectrum, which reveals equivalence of the four ethyl groups and the two Cp* rings, as well as a

Scheme 3

diagnostic high-field Rh–H peak; thus, the formal oxidation state of all three metals is +3 and the metal-bound hydrogen is protonic, as usual in hydridometallacarboranes.^{1,2c,d,12} The monochloro and dichloro derivatives were obtained in amounts too small to permit useful NMR study and were characterized by mass spectroscopy only.

In order to further extend this family of tetradecker sandwiches, we combined the iridacarborane and cobaltacarborane double-decker complex anions **2c**[−] and **4b**[−] with Rh³⁺ in an effort to obtain a heterotrimetallic Co–Rh–Ir “group9ocene” sandwich (Scheme 3). Not surprisingly, this three-way reaction (reminiscent of the “combinatorial synthesis” approach now in vogue) proved quite complicated and generated a large number of products, which varied not only in metal content but also in the number of chloro substituents. As a main objective, we focused on isolating a Co–Rh–Ir complex, and chromatography of the product mixture in several stages eventually produced a fraction from which a small quantity of the dichloro species Cp*Co(Et₂C₂B₃H₂Cl)RhH(Et₂C₂B₃H₂Cl)IrCp* (**7**) was isolated and characterized via NMR, UV–visible, and mass spectroscopy. Other complexes corresponding to [Cp*Co(Et₂C₂B₃H₂-Cl)]₂RhH (**8**) and the previously described [Cp*Ir(Et₂C₂B₃H₂-Cl)]₂RhH (**6**) were also identified. Compound **8** and its parent (nonhalogenated) counterpart have been prepared and structurally characterized in earlier work,^{6c} details of which will be presented elsewhere.

The mass spectrum of **7** exhibits a strong parent group at *m/z* 931 (base peak), as well as less intense groups near *m/z* P – 35 and P + 35, corresponding to monochloro and trichloro derivatives, respectively. That the latter compounds are products of the reaction, and not just species generated from **7** in the mass spectrometer, was demonstrated by further chromatographic work which produced nearly spectroscopically pure samples; unfortunately, the quantities of these substances were insufficient for further characterization.

The proton NMR spectrum of **7** in CDCl₃ supports the proposed tetradecker structure; thus, the Cp* peaks at δ 1.60 and 1.73 are readily assigned to Cp*Co and Cp*Ir, respectively, since they correlate closely with the spectra of **8** (δ_{Cp*Co} = 1.57) and **6** (δ_{Cp*Ir} = 1.74). Similarly, the ethyl CH₃ triplets at δ 1.43 and 1.21 can be correlated with the corresponding signals at δ 1.37 and 1.27 in the spectra of **8** and **6**, respectively. The broad high-field peak at δ –2.8 is assigned to the Rh–H group, although some degree of Ir–H and/or Co–H interaction involving proton migration between Rh and the other metal centers cannot be ruled out. Although microcrystal **7** was

obtained, we have thus far been unable to grow X-ray-quality crystals of this compound.

Conclusions

This work extends the synthetic approach employed in cobaltacarborane sandwich complexes to the heavier group 9 metals and establishes that the same general structural principles apply to species containing iridium and/or rhodium. As with the cobalt sandwiches, the heavy-metal tetradecker analogues are intensely colored air-stable solids, soluble in organic solvents, and from limited observation appear to undergo similar halogenation reactions. Previously noted trends in electronic structure are also further extended in these compounds, but it remains to be seen whether the electrochemical behavior of the rhodium and iridium multidecker sandwiches will parallel that of their cobalt (and other first-row-metal) counterparts; this is among the questions to be addressed in continuing investigations in this area.

Experimental Section

Instrumentation. ^1H NMR spectra (300 MHz) and ^{11}B NMR spectra (115.8 MHz) were recorded on GE QE-300 and Nicolet NT-360 spectrometers, respectively. Unit-resolution mass spectra were obtained on a Finnegan MAT 4600 spectrometer using perfluorotributylamine (FC43) as a calibration standard. In each case, a strong parent envelope whose intensity pattern was consistent with the calculated spectrum based on natural isotopic abundances was observed. Elemental analyses were conducted on a Perkin-Elmer 2400 CHN analyzer using 2,4-dinitrophenylhydrazine as a standard. For unexplained reasons, several of the chlorinated compounds did not give satisfactory combustion analyses. Visible-ultraviolet spectra were recorded on a Hewlett-Packard 8452A diode array spectrophotometer with an HP Vectra computer interface. ^1H and some ^{11}B NMR data for new compounds are listed in Table 1.

Materials and Procedures. All reactions were conducted under an inert atmosphere unless otherwise indicated. Workup of products was generally carried out in air using benchtop procedures. Column chromatography was performed on silica gel 60 (Merck) or neutral alumina. Solvents were distilled from appropriate drying agents under an inert atmosphere. $(\text{Cp}^*\text{IrCl}_2)_2$ was prepared by the literature method,¹⁴ and all other chemicals were of reagent grade and were used without further purification. We thank the Johnson-Matthey Corp. for a generous loan of $\text{IrCl}_3 \cdot x\text{H}_2\text{O}$.

Synthesis of $\text{Cp}^*\text{Ir}(\text{2,3-Et}_2\text{C}_2\text{B}_4\text{H}_4)$ (1a) and $\text{Cp}^*\text{Ir}(\text{2,3-Et}_2\text{C}_2\text{B}_4\text{H}_3\text{-4-Cl})$ (1b). (a) **From the Carborane Dianion.** A 125-mL Schlenk flask equipped with a stir bar and rubber septum was evacuated, filled with N_2 , and charged with 40 mL of THF. To this was added 1.3 equiv of $\text{2,3-Et}_2\text{C}_2\text{B}_4\text{H}_6$ (215 mg, 1.63 mmol) via syringe. The flask was cooled to 0 °C, and 2.6 equiv of *tert*-butyllithium (1.9 mL of 1.7 M solution in hexanes) was added, producing a dark orange color that faded to yellow. The septum was removed under N_2 flow, and 1.0 equiv of $(\text{Cp}^*\text{IrCl}_2)_2$ (0.500 g, 1.26 mmol Ir) was quickly added. The flask was fitted with a reflux condenser, and the contents were purged with N_2 for 15 min and heated to reflux under N_2 . Before reflux began, the stirred orange suspension of $(\text{Cp}^*\text{IrCl}_2)_2$ had cleared to a transparent orange solution. Following 1 day of reflux, the light orange-yellow solution was cooled to room temperature, the solvent was removed under vacuum on a Schlenk line, and the yellow residue was extracted with three 20-mL portions of warm hexane, each extract being cannula-filtered into a second N_2 -filled flask. Evaporation of solvent from the combined extracts yielded yellowish-white crystals, from which the yellow impurity was removed by six successive 5–10 mL washes with hexane at –78 °C. The cold hexane extracts were reserved for later recovery of additional product via chromatography on silica.

The colorless product material was redissolved in 40 mL of hexane, forming a turbid solution, which was removed from the flask via syringe and passed through a syringe filter (Whatman GD/X 13 mm, 0.45 μm ,

Nylon) into a clean flask. The hexane was then removed under vacuum to yield 96 mg (17%) of colorless crystalline **1a**.

In preparations where the 4-chloro derivative **1b** was shown by mass spectroscopic analysis to be present, the compounds were separated by chromatography on silica TLC plates in 5% THF in hexane, using a UV detector, or by preparative-scale HPLC with UV detection at 250 nm. Owing to band overlap, two passes were required to obtain pure material.

(b) **From the Carborane Monoanion.** A 250-mL Schlenk flask equipped with a stir bar and rubber septum was evacuated, filled with N_2 , and charged with 40 mL of THF. To this was added 1.0 equiv of $(\text{Cp}^*\text{IrCl}_2)_2$ (0.562 g, 1.41 mmol Ir). A solution containing 2.0 equiv of the $\text{Et}_2\text{C}_2\text{B}_4\text{H}_5^-$ monoanion was prepared in a second flask by injecting 0.37 g (2.82 mmol) of the neutral carborane into a suspension of dry NaH in THF, stirring until effervescence ceased, and then allowing the suspension to settle for 0.5 h. This solution was transferred to the stirred suspension of the $(\text{Cp}^*\text{IrCl}_2)_2$ by slow cannula filtration over a 30 min period. Toward the end of this procedure, the orange suspension cleared and the solution darkened to a reddish orange. The mixture was refluxed under N_2 for 2.5 d, during which the solution became a lighter yellow-orange.

After the mixture had cooled, the solvent was removed under vacuum, leaving concentric rings of white and yellow material on the walls. To extract the yellow impurity, the flask was pumped to dryness over 1 h and refilled with N_2 , and 15–20 mL of hexane was then added. After the mixture was chilled to –50 °C while being stirred, the hexane was withdrawn by cannula filtration into a second flask. This extraction was repeated, and the combined golden-orange extracts were rotary-evaporated to a red oil which showed signs of decomposing in air; this material was not further examined. Hexane (30 mL) was added to the nearly white residue from the cold hexane extractions, and the solution was warmed, stirred, and cannula-filtered into a round-bottom flask open to the air. After three such warm hexane extractions, the combined pale yellow filtrates were rotary-evaporated to give white crystals that were contaminated on their fringes by yellow material. NMR and TLC analysis of this material showed it to be a roughly equal mixture of **1a** and **1b**. The yield of the combined products was 0.338 g (50%). The desired product **1a** was purified by plate TLC or HPLC on silica using 5% THF in hexane. MS base peaks (molecular ion envelope): for **1a**, m/z 457; for **1b**, m/z 493. UV–visible absorption for **1a** (nm): 232 ($\epsilon = 36\,000\text{ cm}^{-1}\text{ M}^{-1}$). ^{13}C NMR for **1a** (75.5 MHz, δ , C_6D_6 solution): 89.7 (C_5 ring), 22.6 (ethyl CH_2), 15.0 (ethyl CH_3), 9.8 (Cp^*CH_3). Anal. Calc for **1a**, $\text{IrC}_{16}\text{B}_4\text{H}_{29}$: C, 42.06; H, 6.40. Found: C, 42.03; H, 6.06. Anal. Calc for **1b**, $\text{IrClC}_{16}\text{B}_4\text{H}_{28}$: C, 39.11; H, 5.74. Found: C, 38.71; H, 5.62.

Synthesis of *nido*- $\text{Cp}^*\text{Ir}(\text{Et}_2\text{C}_2\text{B}_3\text{H}_5)$ (2a) and *nido*- $\text{Cp}^*\text{Ir}(\text{Et}_2\text{C}_2\text{B}_3\text{H}_4\text{-4-Cl})$ (2b). For the preparation of pure **2a**, a mixture of 5 mL of TMEDA and 5 drops of water was deaerated by N_2 bubbling for 5 min and was then transferred to a small flask containing 68.2 mg (0.149 mmol) of **1a** and equipped with a stir bar. The mixture was stirred for 2.25 h, although monitoring by TLC (silica strips, 1:1 hexane– CH_2Cl_2) indicated that the reaction was essentially complete after 1.25 h. The contents of the flask were rotary-evaporated to afford a yellow oil; this was taken up in hexane, and the solution was flash-filtered through 3 cm of silica in hexane. Evaporation of the filtrate gave a clear oil (easily overlooked) which upon further evacuation produced a white solid identified as pure **2a**, 57.6 mg (0.128 mmol, 86%). When the same procedure was applied to a mixture of **1a** and **1b**, both **2a** and **2b** were obtained and were separated via chromatography on silica. MS base peaks (molecular ion envelope): for **2a**, m/z 447; for **2b**, m/z 481. UV–visible absorptions for **1a** (nm): 232 ($\epsilon = 31\,000\text{ cm}^{-1}\text{ M}^{-1}$), 266 (shoulder, $\epsilon = 11\,000$). Anal. Calc for **2a**, $\text{IrC}_{16}\text{B}_3\text{H}_{30}$: C, 42.99; H, 6.76. Found: C, 44.29; H, 6.96. Anal. Calc for **2b**, $\text{IrClC}_{16}\text{B}_3\text{H}_{29}$: C, 39.92; H, 6.07. Found: C, 39.49; H, 6.67.

Synthesis of $\text{Cp}^*\text{Ir}(\text{Et}_2\text{C}_2\text{B}_4\text{H}_3\text{-5-Cl})$ (1c), $\text{Cp}^*\text{Ir}(\text{Et}_2\text{C}_2\text{B}_4\text{HCl}_3)$ (1d), and *nido*- $\text{Cp}^*\text{Ir}(\text{Et}_2\text{C}_2\text{B}_3\text{H}_4\text{-5-Cl})$ (2c). (a) **Reaction with Cl_2 .** A 20 mL vial equipped with a stir bar was charged with 131 mg (0.286 mmol) of **1a** and 5 mL of CH_2Cl_2 , and Cl_2 was bubbled through the solution until the color was greenish yellow. The vial was sealed with a septum fitted with a pressure-relief needle, and the contents were stirred, with monitoring every 30 min via TLC silica strips (vide supra). After 30 min, there was evidence of reaction but starting material

remained, so more Cl_2 was added and stirring was continued for 30 min. At this point, TLC analysis indicated the absence of **1a** and the presence of major and minor products. The vial was evacuated overnight, after which NMR and mass spectroscopy revealed that the residue consisted mainly of **1c** and a trace of a dichloro derivative of **1a**. In one experiment involving a higher concentration of Cl_2 , the reaction was complete within 5 min, affording the trichlorinated product **1d**, which was characterized spectroscopically but failed to decap on treatment with TMEDA.

(b) Reaction with *N*-Chlorosuccinimide (NCS). A sample of 379 mg (0.828 mmol) of **1a** in 30 mL of THF was deaerated with N_2 for 15 min, after which 1.5 equiv (169 mg, 1.27 mmol) of NCS was added and the solution heated to reflux under a N_2 atmosphere. The reaction was monitored as before by using TLC strips and pure **1a** as a reference, and it was noted that although the desired **1c** appeared within 30 min, significant **1a** remained after 3 h. Addition of another 80 mg of NCS had little effect, so the reflux was discontinued, 120 mg of NCS was added, and the reaction mixture was stirred at room temperature for 3 h (total of 10 h), resulting in complete consumption of **1a**. The solution was rotary-evaporated, the residue taken up in CH_2Cl_2 , the resultant solution filtered through 3 cm of silica, and the solvent removed to afford white **1c** together with traces of yellowish-brown material.

Decapping of product **1c** was conducted as described above using wet TMEDA. After removal of volatiles under vacuum, the residue was flash-filtered through 2 cm of silica and the filtrate evaporated to give 301 mg (0.625 mmol, 76% based on **1a**) of colorless **2c**. MS base peaks (molecular ion envelope): for **1c**, m/z 493; for **1d**, m/z 562; for **2c**, m/z 481.

Synthesis of $\text{Cp}^*\text{Ir}(\text{Et}_2\text{C}_2\text{B}_3\text{H}_2\text{-4[6-Cl]}\text{IrCp}^*$ (3**).** A solution of 2 equiv of the monoanion of **2a** was prepared via addition of 0.233 mmol of *n*-butyllithium (0.14 mL of 1.6 M in hexanes) to an equimolar amount of **2a** in 40 mL of THF at 0 °C. The solution was warmed to room temperature, and 1 equiv of $(\text{Cp}^*\text{IrCl}_2)_2$ (46 mg, 0.058 mmol) was added under a flow of N_2 . The orange color of the initially formed suspension of $(\text{Cp}^*\text{IrCl}_2)_2$ changed within 15 min to a khaki color, then to red-orange, and within 1 h to a clear orange-brown. The solution was stirred overnight (although the reaction was later shown to reach completion within 3 h), and the mixture was then opened to the air and THF was removed by rotary evaporation. The red residue was taken up in hexane, the resultant solution was flash-filtered through 3 cm of silica, and solvent was removed to yield 52 mg of the **2a** starting material (ca. 50% recovery). The silica was washed with CH_2Cl_2 to give a bright yellow solution which was evaporated to give 38 mg (0.047 mmol, 41% based on Ir consumed) of **3**. Analysis by silica TLC employing a variety of solvent combinations showed no other products. MS base peak (molecular ion envelope): m/z 807. UV-visible absorptions for **1a** (nm): 234 ($\epsilon = 26\,000\text{ cm}^{-1}\text{ M}^{-1}$), 272 ($\epsilon = 41\,000$), 414 ($\epsilon = 1500$), 472 ($\epsilon = 380$). Anal. Calc for $\text{Ir}_2\text{Cl}_2\text{C}_{26}\text{B}_3\text{H}_{42}$: C, 38.70; H, 5.25. Found: C, 40.18; H, 5.65.

Synthesis of $\text{Cp}^*\text{Ir}(\text{Et}_2\text{C}_2\text{B}_3\text{H}_2\text{-4[6-Cl]}\text{CoCp}^*$ (5**).** A solution containing 2.0 equiv of the $\text{Cp}^*\text{Co}(\text{Et}_2\text{C}_2\text{B}_3\text{H}_4)^-$ monoanion was prepared at 0 °C via addition of 0.80 mmol of *n*-butyllithium (0.50 mL of 1.6 M in hexanes) to a stirred solution of 247 mg (0.787 mmol) of **4a** in 30 mL of THF under N_2 . After 15 min of stirring at room temperature, 1 equiv of $(\text{Cp}^*\text{IrCl}_2)_2$ (158 mg, 0.198 mmol) was added under a flow of N_2 . The originally orange suspension changed within 10 min to a deep burgundy red solution. Overnight stirring produced a change to a dark green. The mixture was opened to the air and THF removed by rotary evaporation. The dark residue was taken up in hexane, and the solution was flash-filtered through 3 cm of silica, giving a yellow filtrate from which solvent was removed to yield 123 mg of the **4a** starting material (ca. 50% recovery). The green hexane-insoluble residue was taken up in CH_2Cl_2 , and the solution was flash-filtered through the same silica column. Rotary-evaporation of the filtrate gave 229 mg (0.34 mmol, 87%) of green crystalline **5**. Although TLC analysis with several different solvent mixtures gave no evidence of other products, the sample of **5** was further chromatographed on a silica column in 5% THF in hexane, again affording only **5** (132 mg, 50%).

In a different synthesis intended to check the possibility that the chlorine in **5** was acquired during workup, the above procedure was followed except that 10% THF in hexane was employed in place of CH_2Cl_2 in filtration and chromatography. Again the only product

obtained was **5**, establishing that chlorination occurs during the reaction and the source of the chlorine is the iridium reagent (or species derived from it) rather than solvent. MS base peak (molecular ion envelope): m/z 675. UV-visible absorptions for **1a** (nm): 232 ($\epsilon = 20\,000\text{ cm}^{-1}\text{ M}^{-1}$), 326 ($\epsilon = 38\,000$), 598 ($\epsilon = 630$). Anal. Calc for $\text{IrCoCl}_2\text{C}_{26}\text{B}_3\text{H}_{42}$: C, 46.36; H, 6.28. Found: C, 46.45; H, 6.70.

Synthesis of $[\text{Cp}^*\text{Ir}(\text{Et}_2\text{C}_2\text{B}_3\text{H}_2\text{-5-Cl})_2\text{RhH}$ (6**).** A 1.0-equiv sample of $\text{RhCl}_3(\text{MeCN})_3$ (67 mg, 0.20 mmol) was transferred in a drybox to a 100-mL two-neck flask containing a stir bar, the flask was sealed with rubber septa, and 25 mL of THF was added on a Schlenk line via syringe. In a second two-neck flask, 3.0 equiv (294 mg, 0.61 mmol) of the $\text{Cp}^*\text{Ir}(\text{Et}_2\text{C}_2\text{B}_3\text{H}_3\text{-5-Cl})^-$ monoanion was prepared from **2c** via deprotonation with 0.61 mmol of *n*-butyllithium (0.38 mL of 1.6 M solution in hexanes), which produced a change from nearly colorless to yellow. This solution was transferred via cannula at a rate of 2.5 mL/min to the stirred suspension of $\text{RhCl}_3(\text{MeCN})_3$ at -78 °C in a dry ice/alcohol bath. The reaction mixture was allowed to warm slowly with stirring under N_2 . After 2 h, the temperature was -20 °C and the mixture was reddish-brown; after 18 h, it was dark brown. The reaction was halted and the solvent removed under vacuum, leaving a dark residue which was taken up in 10 mL of toluene. Half of this solution was transferred by syringe under N_2 to the top of a silica column that had been purged with N_2 . The sample was eluted with hexane followed by toluene. The hexane eluate afforded impure **2c** starting material. This, combined with material recovered from the second half of the toluene solution, was purified by plate TLC on silica using hexane to give a total recovery of 87 mg (30%) of **2c**.

The toluene eluate yielded minor yellow and yellow-green bands, which were not characterized, followed by a major green-brown band that comprised at least two overlapping compounds. This band was collected in four fractions whose colors progressed from khaki green to brown. From NMR and mass spectroscopic evidence, the first fraction contained nearly pure, dark green **6**. Spectra for the remaining fractions showed a decrease in the concentration of **6** and an increase in that of a monochlorinated tetradecker product (m/z 1030) corresponding to **6** with loss of one chlorine. The combined yield of both products was 25 mg (24% based on **2c** consumed). Further chromatography on these fractions employing 14% THF in hexane produced additional **6**, monochloro complex, and a trichloro tetradecker (m/z 1099). MS base peak for **6** (molecular ion envelope): m/z 1064. UV-visible absorptions for **6** (nm): 232 ($\epsilon = 9000\text{ cm}^{-1}\text{ M}^{-1}$), 320 ($\epsilon = 20\,000$).

Synthesis of Mixed-Metal Tetradecker Sandwiches from the $\text{Cp}^*\text{Co}(\text{Et}_2\text{C}_2\text{B}_3\text{H}_3\text{Cl})^-$ and $\text{Ir}^*\text{Co}(\text{Et}_2\text{C}_2\text{B}_3\text{H}_3\text{Cl})^-$ Substrate Anions. A suspension of 100 mg (0.301 mmol) of $\text{RhCl}_3(\text{MeCN})_3$ in 20 mL of THF in a 250-mL Schlenk flask was stirred at -78 °C. In a separate two-neck, 100-mL round-bottom flask were placed 118 mg (0.339 mmol) of $\text{Cp}^*\text{Co}(\text{Et}_2\text{C}_2\text{B}_3\text{H}_4\text{-5-Cl})$ (**4b**) and 283 mg (0.588 mmol) of $\text{Cp}^*\text{Ir}(\text{Et}_2\text{C}_2\text{B}_3\text{H}_4\text{-5-Cl})$ (**2c**); this flask was evacuated with heating, after which it was filled with N_2 and 20 mL of THF was added. The flask was placed in a 0 °C bath, and 0.928 mmol of *n*-butyllithium (0.58 mmol, 1.6 M in hexanes) was added. After 15 min of stirring, the flask was warmed to room temperature and the contents were stirred for an additional 30 min. This solution of mixed metallacarborane monoanions was transferred via cannula to the Schlenk flask containing the $\text{RhCl}_3(\text{MeCN})_3$, using a slow drip rate over a 40-min period. After the transfer was complete, 8 mL of THF was added to the two-neck monoanion flask, and this rinsing was also transferred to the Schlenk flask. Even at -78 °C, the mixture darkened noticeably as the suspended Rh complex entered the reaction. The reaction mixture was permitted to warm to room temperature with stirring over a 4 h period, after which it was stirred another 30 min. At this point, the mixture had acquired a rich dark brown color.

For workup, the reaction mixture was divided into two portions, A and B, for which different procedures were followed. Portion A, comprising about one-third of the original mixture, was transferred to a round-bottom flask and rotary-evaporated to give a dark oil, which was extracted with hexane, leaving much dark brown insoluble material. The hexane extract was flash-filtered through 3 cm of silica, which after evaporation gave 73 mg of a pale yellow material that proved on NMR analysis to be a mixture of the **4b** and **2c** starting materials. The hexane-insoluble portion was extracted with toluene, and the extract

was flash-filtered, yielding a rich brown filtrate which was rotary-evaporated to afford 10 mg of a dark brown crystalline material. This sample was redissolved in toluene, and the solution was chromatographed on a 32-cm silica column prepared from a toluene slurry, using toluene as eluent. This produced 12 distinct but overlapping bands, the first two of which were yellow **4b** and orange **2c**, followed by several khaki to dark brown bands. Of these, the most intensely colored, and most abundant, was dark brown **8**, a known^{6c} Co–Rh–Co tetradeccker complex (parent envelope m/z 796). Following the dark bands were a series of four diffuse orange bands, the second of which (ninth in the overall sequence) exhibited a mass spectrum (parent envelope m/z 931) assigned to the dichloro Co–Rh–Ir tetradeccker **7**. Further purification of this material by TLC on a silica plate in 3:2 hexane–CH₂Cl₂ produced an additional band, tan in color, which moved faster than **7** on the plate and was identified by mass spectroscopy (parent envelope m/z 964) as a trichloro Co–Rh–Ir tetradeccker, i.e., compound **7** with an additional chlorine substituent.

Portion B of the product mixture was worked up as follows. After removal of solvent in vacuo, the residue was extracted with CH₂Cl₂ under N₂ and the extract was flash-filtered through 3 cm of Celite, which removed some tan debris and produced a dark chocolate-colored filtrate. To this 75 mL solution was added 40 mL of hexane, and the mixture was rotary-evaporated to remove most of the CH₂Cl₂, leaving a dark residue “C”. The dark supernate was flashed through 3 cm of silica with hexane, and the solvent was stripped to yield 154 mg of lemon-yellow solid which was shown by NMR to consist mainly of recovered **4b** and **2c**. The silica filter bed was then flushed with CH₂Cl₂ to produce a dark brown filtrate, which was evaporated to dryness to give 130 mg of dark solid “D”. Samples C and D were separately chromatographed on silica in toluene, each producing six to eight bands which were analyzed by mass spectroscopy and found to contain a variety of apparent triple-decker and tetradeccker complexes with varying combinations of the three metals employed in the reaction and different numbers of chlorine substituents, most of which were not further investigated. Since the main species of interest was the heterotrimetallic dichloro compound **7**, the main effort was directed toward collecting

this material and its trichloro derivative for spectroscopic characterization. UV–visible absorptions for **7** (nm): 232 ($\epsilon \sim 27\,000\text{ cm}^{-1}\text{ M}^{-1}$), 262 ($\epsilon \sim 23\,000$), 368 ($\epsilon \sim 40\,000$).

X-ray Structure Determinations of **1a and **3**.** Diffraction data were collected on a Rigaku AFC6S diffractometer at $-120\text{ }^\circ\text{C}$ using Mo K α radiation. Details of the data collection and structure determination are listed in Table 2. The unit cell dimensions were determined by least-squares refinement of the setting of 25 high-angle reflections. The intensities of three standard reflections, monitored at 3-h intervals, showed no significant variation. Empirical absorption corrections were applied following ψ scanning of several reflections (transmission factors are reported in Table 2). All calculations were performed on a VAX station 3500 computer employing the TEXSAN 5.0 crystallographic software package¹⁵ and in later stages on a Silicon Graphics Personal Iris 4D35 computer with the teXsan 1.7 package.¹⁶ The structure was solved by direct methods in SIR88.¹⁷ High thermal parameters observed for the triple-decker structure indicated possible disorder, but efforts to resolve this disorder were unsuccessful.

Acknowledgment. This work was supported by the U.S. Army Research Office, Grant No. DAAH04-95-1-0145, and the National Science Foundation, Grant No. CHE 9322490. We thank Eric Boring for obtaining many of the elemental analyses.

Supporting Information Available: Tables of atomic coordinates, anisotropic thermal parameters, and calculated mean planes for **1a** and **3** (6 pages). Ordering information is given on any current masthead page.

IC9606587

-
- (15) TEXSAN 5.0: Single Crystal Structure Analysis Software (1989), Molecular Structure Corp., The Woodlands, TX 77381.
 - (16) teXsan 1.7: Single Crystal Structure Analysis Software (1995), Molecular Structure Corp., The Woodlands, TX 77381.
 - (17) SIR88: Burla, M. C.; Camalli, M.; Cascarano, G.; Giacovazzo, C.; Polidori, G.; Spagna, R.; Viterbo, D. *J. Appl. Crystallogr.* **1989**, *22*, 389.